

An ANN Based Sensitivity Analysis of Factors Affecting Stability of Gravity Hunched Back Quay Walls

Karimnader-Shalkouhi S. ^{a*}, Karimpour-Fard M. ^a, Machado S. L. ^b

^a University of Guilan, Rasht, Guilan, Iran.

^b Dept. of Materials science and technology, Federal University of Bahia., Salvador-BA, Brazil.

Received 16 April 2017; Accepted 20 May 2017

Abstract

This paper presents Artificial Neural Network (ANN) prediction models that relate the safety factors of a quay wall against sliding, overturning and bearing capacity failure to the soil geotechnical properties, the geometry of the gravity hunched back quay walls and the loading conditions. In this study, a database of around 80000 hypothetical data sets was created using a conceptual model of a gravity hunched back quay wall with different geometries, loading conditions and geotechnical properties of the soil backfill and the wall foundation. To create this database a MATLAB aided program was written based on one of the most common manuals, OCDI (2002). Comparison between the results of the developed models and cases in the data bank indicates that the predictions are within a confidence interval of 95%. To evaluate the effect of each factor on these values of factor of safety, sensitivity analysis were performed and discussed. According to the performed sensitivity analysis, shear strength parameters of the soil behind and beneath the walls are the most important variables in predicting the safety factors.

Keywords: Quay Wall; Hunched Back; Safety Factor; Sliding; Overturning; Bearing Capacity; Artificial Neural Network.

1. Introduction

Gravity quay walls are one of the most common port and harbor structures because of their applicability (e.g., ship-loading, supporting facilities on their backfill, optimizing access to land, and navigable waters), durability, ease of construction, and the possibility of deep construction and reaching deep seabed elevations. However, because of the considerable weight of the wall's sections, some issues exist regarding the stability of their foundations. During previous earthquakes, gravity quay walls have suffered significant damage as a result of their seaward movement and this has led to subsequent damage to the structures built on their backfill [1].

According to Figure 1, compared to a vertical-back wall, a landward-leaning wall has a smaller failure wedge and therefore a smaller lateral thrust to retain. But, a larger failure wedge and lateral thrust develop behind a seaward (for quay walls) leaning wall. However, in comparison to the more common vertical-back walls, a large landward-leaning gravity wall would be considerably more expensive as it would require a significant amounts of material (e.g., concrete and steel reinforcement) to construct, may have soil bearing capacity problems attributable to its heavier weight, and because of its larger mass, greater inertial forces are applied on it during earthquakes [2].

* Corresponding author: samirakarimnader@yahoo.com

➤ This is an open access article under the CC-BY license (<https://creativecommons.org/licenses/by/4.0/>).

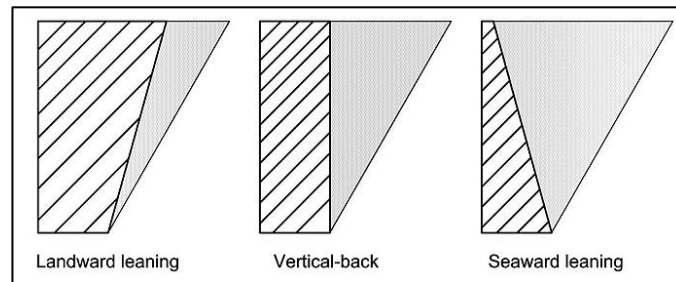


Figure 1. Types of wall rear-face shapes (hatched: wall; stippled: backfill soil failure wedge), After Sadrekarimi [3]

To overcome these limitations while taking advantage of the reduced lateral earth pressures on the landward-leaning rear face of the wall, a broken-back or hunched back wall is introduced (Figure 2). In a broken-back wall, increasing lateral earth pressures at deeper elevations of the wall are reduced by the landward-leaning rear face of the wall while the cost, weight, and mass of the wall are reduced by using a seaward leaning rear face at shallower elevations where lateral earth pressures are smaller [2, 3].

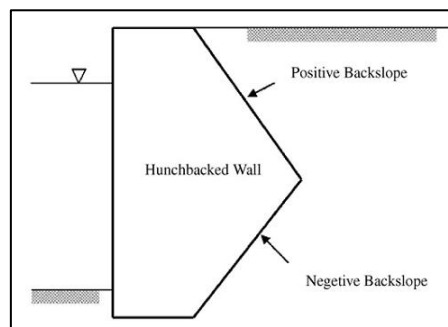


Figure 2. Definitions of negative and positive back-slopes

Reduction of the lateral thrust to the wall by means of changing the wall’s geometry not only increases factor of safety for overturning and sliding, but could also overcome problems related to the bearing capacity of the foundation.

In Figure 3. the results of physical modeling tests by means of shaking table conducted by Sadrekarimi (2010) [4], both in static and dynamic conditions, can be observed. As can be seen, changing the backslope angle from positive to negative leads to a reduction in applied thrust on the quay wall.

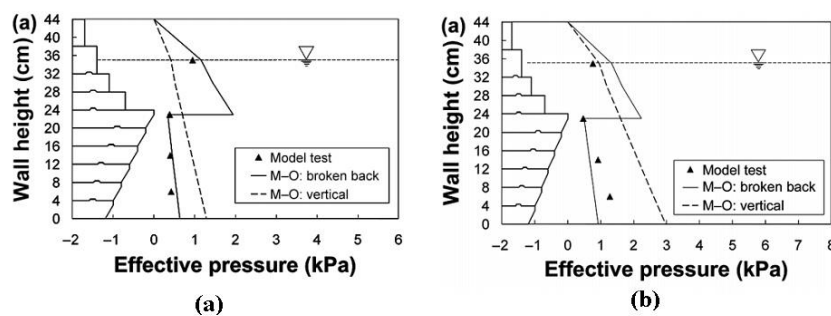


Figure 3. Results of physical modeling tests: effective lateral pressure distributions, measured and calculated by the Mononobe-Okabe model, M-O, acting on the walls in (a) static and (b) dynamic conditions (after Sadrekarimi (2010) [4])

It should be noted that during earthquakes, four different scenarios are considered for the stability analysis of gravity quay walls. These categories include rigid walls retaining dry backfills (Case 1), and three categories for rigid walls retaining submerged backfills, depending upon the magnitude of excess pore water pressures that are generated during the earthquake. They range from the case of no excess pore water pressures (Case 2) to the extreme case which corresponds to the complete liquefaction of the backfill (Case 4) and the intermediate case between the two (Case 3).

Since in practice generally highly permeable granular materials in compacted state are employed as the backfill of quay walls, it has been assumed that the probability of excess pore pressure generation during earthquakes is very low and has a minor effect on the shear strength of the soil behind the quay wall.

1.1. Loads Acting on Hunched Back Gravity Quay Wall

According to the methodology procedure proposed by “Technical Standards and Commentaries for Port and Harbor Facilities in Japan”, OCDI (2002) [5], the external forces and loads which should be considered on a hunched back gravity quay wall for stability analysis are as follows:

- (1) Surcharge
- (2) Deadweight of the wall
- (3) Earth pressure in static and dynamic conditions
- (4) Dynamic water pressure during an earthquake

The surcharge due to the live load of container should be considered for stability analysis. The minimum value of this live surcharge is 1.5 t/m^2 , which could be increased up to 5.5 t/m^2 .

In many types of gravity quay walls, some part of this backfill acts as self-weight of the quay wall, and the portion of the backfill can be considered as a part of the quay wall body. However it is difficult to apply this concept to all cases unconditionally, because the extent of backfill considered as a part of the quay wall body varies depending on the shape of the quay wall body and the mode of failure. However, it is common practice to define the extent of backfill considered as a part of the quay wall body as shown by hatching in Figure 4 [5].

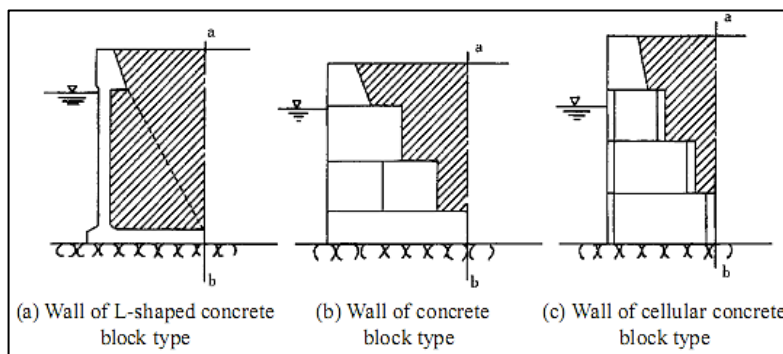


Figure 4. Determination of Quay wall Body

Okabe (1924) [6] and Mononobe and Matsuo (1929) [7] extended Coulomb's theory of static active and passive earth pressures to include the effects of dynamic earth pressures on retaining walls (Figure 5). The Mononobe-Okabe theory, M-O, incorporates the effect of earthquakes through the use of a constant horizontal acceleration in units of g , $a_h = k_h \cdot g$, and a constant vertical acceleration in units of g , $a_v = k_v \cdot g$, acting on the soil mass comprised of Coulomb's active wedge (or passive wedge) within the backfill, however the vertical component of acceleration is generally neglected.

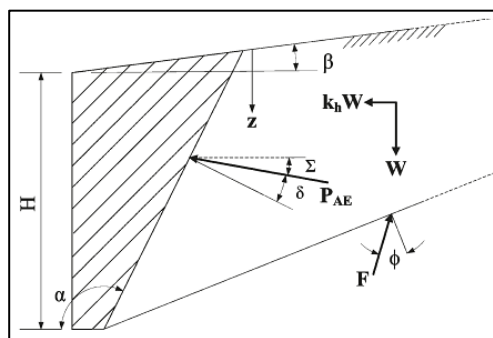


Figure 5. Forces acting on the active failure wedge in M-O analysis

In the M-O method, the horizontal effective active pressure acting on a wall with a cohesionless backfill is calculated as follows:

$$P_{AE} = K_{AE} \gamma_{sub} z \cos \Sigma \tag{1}$$

Where K_{AE} is the pseudo-static seismic active earth pressure coefficient, γ_{sub} is the submerged unit weight of the backfill soil, z is the soil depth, and Σ is defined below. Figure 5. shows the active force, P_{AE} , on a schematic wall during an earthquake and the parameters of equation 1. According to this figure, α and $\Sigma (= \alpha - \delta - 90^\circ)$ are the inclinations of the wall's rear face and P_{AE} from horizontal, respectively, and δ is the interface friction angle between the wall and the backfill soil, which is about 50% of the internal friction angle of the backfill soil, ϕ [1, 4, 8].

K_{AE} is the pseudo-static seismic active earth pressure coefficient defined as follows:

$$K_{AE} = \frac{\sin^2(\alpha - \theta + \varphi)}{\cos\theta \sin^2\alpha \sin(\alpha - \theta - \delta) \left[1 + \sqrt{\frac{\sin(\varphi + \delta) \sin(\varphi - \beta - \theta)}{\sin(\alpha - \theta - \delta) \sin(\alpha + \beta)}} \right]^2} \quad (2)$$

Where β is the backfill slope angle (assumed nil in our analyses), and θ is the apparent seismic angle defined as follows:

$$\theta = \tan^{-1} \left[\frac{G_s}{G_s - 1} k_h \right] \quad (3)$$

Where G_s is the specific gravity of backfill soil particles [6, 7].

The hydrodynamic water pressure force for the free water within the backfill is given by the Westergaard (1931) relationship:

$$P_{wd} = \frac{7}{8} k_h \gamma_w \sqrt{y_w H_p} \quad (4)$$

Where y_w is the depth of water and H_p is the total depth of the water. The resultant dynamic water pressure force, P_{wd} , is equal to:

$$P_{wd} = \frac{7}{12} k_h \gamma_w H_p^2 \quad (5)$$

This force acts at an elevation equal to $0.4H_p$ above the base of the pool as shown in Figure 6.

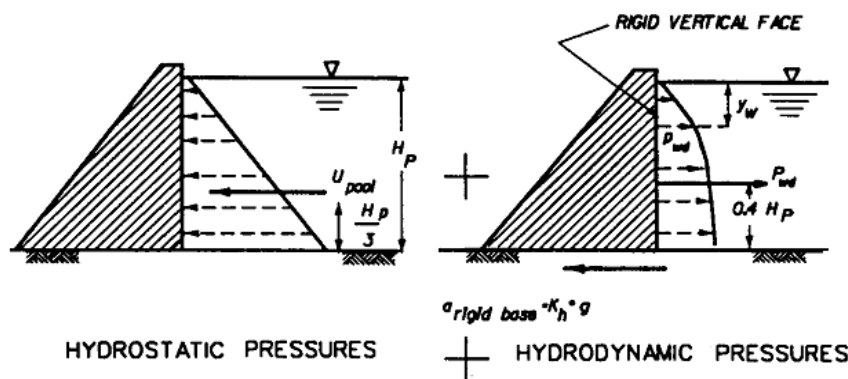


Figure 6. Hydrostatic and Hydrodynamic pressure

As the excess pore pressures are positive in front of wall and negative behind it, the total hydro-dynamic pressure acting on the submerged wall is twice that given by the Westergaard equation [9].

1.2. Stability Calculations

Based on the Technical Standards and Commentaries of Port and Harbor Facilities in Japan, OCDI (2002), in the stability calculations of a gravity type quay wall, the following items should be examined in general:

- Sliding of the wall
- Bearing capacity of the foundation
- Overturning of the wall

The safety factor against sliding of a gravity type quay wall shall be calculated using Equation 6.

$$F_s = \frac{fW}{P} \quad (6)$$

Where W is the resultant vertical force acting on the wall (kN/m), P , the resultant horizontal force acting on the wall (kN/m), f , the coefficient of friction between the bottom of the wall body and the foundation and F_s is the safety factor. The safety factor should be 1.2 or more in ordinary conditions and 1.0 or more in extraordinary conditions.

The circular arc analysis is used as a standard method to examine the bearing capacity of the quay wall's foundation subjected to eccentric and inclined loads. The circular arc analysis based on the simplified Bishop method

has been used in this case. The safety factor should be at least 1.2 in ordinary conditions and 1.0 in extraordinary conditions.

The safety factor against the overturning of gravity type quay wall shall satisfy Equation 7.

$$F_s = \frac{Wt}{Ph} \tag{7}$$

Where t is distance between the line of application of the resultant vertical forces acting on the quay wall and the front toe of the quay wall and h is height of the application line of the resultant horizontal forces acting on the quay wall, above the bottom of the quay wall. In this case the safety factor should be 1.2 or more in ordinary conditions and 1.1 or more in extraordinary conditions [5].

2. Method

2.1. Conceptual Model

Figure 7. shows a conceptual model of a gravity hunched back quay wall. As illustrated in this figure, geometry of the wall could be described properly through positive and negative angles of the wall's back, and the width of the wall at the top and bottom and the height of the wall.

The free board of the wall which is the distance between the water level and the top of wall is shown by a α factor and the embedment depth of the wall has been shown by a β factor. As could be observed in Figure 7, it is assumed that the level of water behind and in front of the quay wall is equal, thus creating no extra thrust on the wall as a result of water. It was assumed that the width of the wall at the top is 90% the wall's thickness at the bottom. This reduction helps in reducing the weight of wall and also lowers stress concentration in the foundation. Water depth is denoted with H and the surcharge acting on the ground behind the wall is shown with q . There is no doubt that the geotechnical properties of the soil behind and beneath the wall affect the stability of wall so in this conceptual model these parameters should be introduced as a part of the soil-wall system.

As it was mentioned earlier in gravity quay walls in order to prevent the generation of excess pore pressure mainly due to seismic loads, permeable materials in a compacted state are generally employed. In the case of foundations with low bearing capacity, a layer of the same granular materials is also used as the mattress layer. Therefore, the state of stress in this part of the soil-wall system is effective. However, the state of stress in the soil beneath the wall could be either total or effective depending on the soil type. Here in this conceptual model, it is assumed that the backfill materials are always granular with no cohesion but the soil beneath the foundation of the quay wall could be either granular or cohesive. In the case of granular material only internal friction angle as the shear strength parameter was considered. However, in the case of cohesive soils assuming short term stability, undrained shear strength parameter, C_u , was taken for analysis.

In addition to all the variables mentioned, in order to consider the stability of the wall under seismic loading by pseudo static analysis, the horizontal pseudo static coefficient, k_h , was applied.

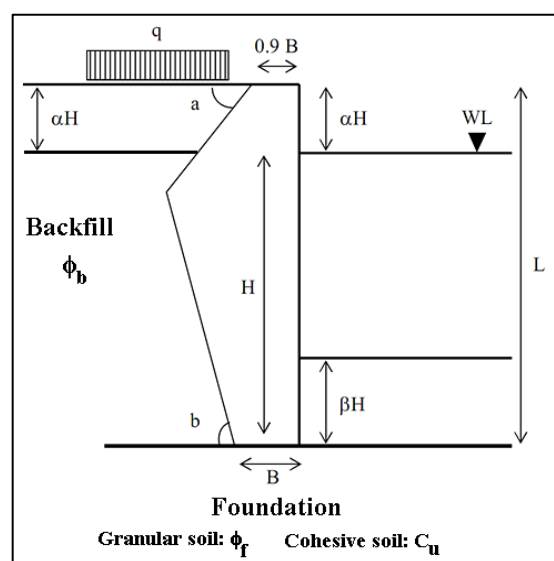


Figure 7. Employed conceptual model of a gravity hunched back quay wall

Table 1. gives the descriptive statistics of the variables used for modeling the safety factors of the wall against sliding, overturning and bearing capacity failure.

Table 1. Descriptive statistics of the variables used in ANN models

Parameter	C_u (kPa)	φ_f (degree)	φ_b (degree)	q (kN/m)	k_h	a (degree)	b (degree)	α	β	H (m)	L/B
Minimum	200	25	35	0	0	60	45	0.1	0	5	2
Maximum	800	35	45	55	0.2	89.9	75	0.2	0.2	10	4
Mean	466.67	30	40	23.33	0.1	74.97	60	0.15	0.1	7.5	3
Standard Deviation	249.45	4.08	4.08	23.21	0.082	12.21	12.25	0.05	0.08	2.04	0.82

2.2. Database

Using the conceptual model from the last section and introducing variables with the range shown in Table 1, hypothetical hunched back gravity walls were created and their stability investigated. The availability of more data can allow to further improve the models to better represent the system. To this aim and in order to capture the full range of the input variables, a large database containing more than 80000 hypothetical cases was created. To facilitate the stability analysis of this number of hypothetical cases, the methodology reviewed in the last section was programmed in MATLAB R2012b (8.0.0.783).

Based on the performed calculations, the database was compiled and employed in modeling the safety factors of gravity walls against sliding, overturning and bearing capacity failure.

The compiled database contains values of undrained cohesion, friction angle of the soil beneath the quay wall (C_u , φ_f), the friction angle of backfill (φ_b), horizontal pseudo static coefficient (k_h) and the geometry of the wall as inputs, whereas the safety factors of the wall against sliding, overturning and bearing capacity failure are entered as outputs. This database was created with the aim of developing models which can be used for an easy preliminary estimation of the stability of quay walls. Generally in the preliminary stage of gravity quay wall design, the geometry of the wall needed to meet the stability criteria is unknown. Achieving the minimum required dimensions of the quay wall to satisfy stability requirements which also leads to the minimum construction material and labor is the main aim of developing such models. After obtaining a preliminary geometry of the quay wall, a more sophisticated analysis could then be performed.

2.3. Modelling Method

The Artificial Neural Networks were employed to develop the prediction models. To evaluate the importance of each factor on the prediction models a set of sensitivity analysis have been performed.

Artificial neural networks are information-processing systems whose architectures essentially mimic the biological system of the brain [10]. ANNs have been successfully applied to link independent variables to a series of dependent ones, mainly where it is diverse to establish numerical equations. The use of ANNs has increased during last decades in various fields of geotechnical engineering such as liquefaction [11, 12], foundation settlements [13], reinforced soil [14] and compaction characteristics of soils [15, 16]. In this study, a multilayer perceptron network has been utilized to present prediction models.

A multilayer perceptron (MLP) is a feed-forward artificial neural network model that maps sets of input data onto a set of appropriate outputs. MLP utilizes a supervised learning technique called back-propagation for training the network. In the application of MLP, data are categorized as input layer, output layer and one or more hidden layers. The input patterns are fed to the network for feed-forward computations to calculate output patterns. The output patterns are compared with corresponding output patterns and the summation of the square of the errors is calculated. The errors are then back propagated through the network using the gradient-descent rule to modify the weights and minimize the summed squared errors. Figure 2. illustrates the typical ANN structure and the relation between input and output parameters.

In this study, a MLP network consisting of three hidden layers with respectively nine, ten and one neurons for the first, second and third hidden layers have been used. The number of neurons in the hidden layer was determined by training several networks with different numbers of hidden neurons and comparing the predicted results with the desired output.

Since the way that the database is used in the training and testing sets has a significant effect on the results, the database was divided into several combinations of training and testing sets until a robust representation of the whole population was achieved. To select an optimal combination of training and testing sets, a statistical analysis considering the maximum, minimum, mean, and standard deviation was performed on the input and output

parameters. The aim of the analysis was to ensure that the statistical properties of the data in each of the subsets were as close to each other as possible and therefore they represented the same statistical population [17].

Sensitivity analysis concerns the mathematical model representation of a physical system and attempts to evaluate the sensitivity of the output patterns to variations of input patterns. The main issues in designing methods for regression sensitivity analysis are the choice of perturbation scheme and the way to assess and measure any influence. An appropriate method for perturbation is to delete observations individually or in groups. This approach is known as case-deletion and it aims to assess the influence of an observation on the final results.

In this research, the type of sensitivity analysis was ANN based. At first a MLP network was trained in the case of each parameter with all data. In the trained network, each neuron in a specific layer is connected to other neurons via weighted connections in which scalar weights show the strength of the connections. In the second step, one of the inputs is removed from the ANN model by setting its scalar weight to zero and then the output is obtained. In this way, all the weighted connections between this variable and other variables will be dropped from the model and therefore the effect of removed input on the prediction of outputs could be pictured.

2.4. Evaluation Method

Different statistical approaches have been used to evaluate the performance of the prediction models. These parameters are the coefficient of determination (*COD*), root mean square error (*RMSE*) and the coefficient of residual mass (*CRM*). The following equations are the mathematical expressions of these parameters:

$$COD = 1 - \frac{\sum_{i=1}^n (M_i - P_i)}{\sum_{i=1}^n (M_i - \bar{M})} \quad (8)$$

$$RMSE = \sqrt{\frac{\sum_{i=1}^n (P_i - M_i)^2}{n}} \times 100 \quad (9)$$

$$CRM = 1 - \frac{\sum_{i=1}^n (P_i)}{\sum_{i=1}^n (M_i)} \quad (10)$$

Where M_i is the actual value and P_i the predicted value, \bar{M} the mean of the actual data and n is the number of data. The *RMSE* is the variance of the residual error, and should be minimized when the outputs fit a set of data. In the case of a perfect fitting, the *RMSE* is zero. The lower the *RMSE*, the higher the accuracy of the model predictions. The coefficient of residual mass, *CRM*, represents the difference between the actual data and the predicted values. The optimum value of *CRM* is zero. Positive values of *CRM* indicate underestimation and vice-versa.

3. Results and Discussions

3.1. ANN Prediction Models for Safety Factors of Quay Walls in Undrained Conditions

Eleven input variables were used for modeling the safety factors of quay walls against sliding, overturning and bearing capacity failure in undrained conditions, including undrained cohesion (C_u), friction angle of the backfill (φ_b), surcharge (q), horizontal pseudo-static coefficient (k_h), water depth (H), L/B , B , a , b , α and β . Hence, the input layers have eleven neurons and the output layers have one neuron. Among the employed data sets, 90% have been used for training and 10% have been used for testing the model.

The models are validated using values from the database. Figures 8 to 10. show comparison between the predicted values of safety factors from model training and testing versus the actual data obtained from deterministic stability analyses. It is clear from the graphs that the MLP models give reliable estimation of the safety factors against sliding and overturning, while concerning bearing capacity failure, the predicted safety factors are generally overestimated.

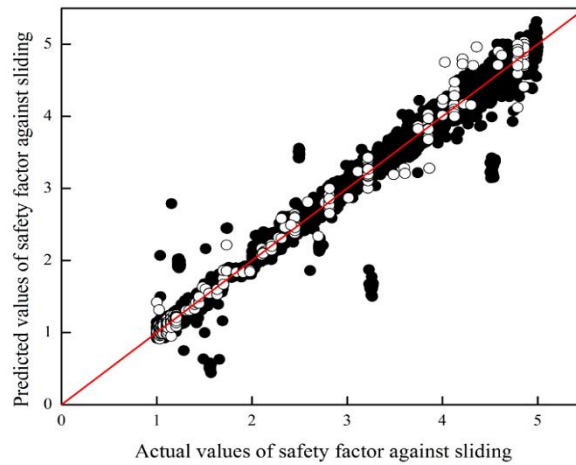


Figure 8. Predicted safety factors against sliding compared to actual values obtained from deterministic stability analyses (undrained conditions)

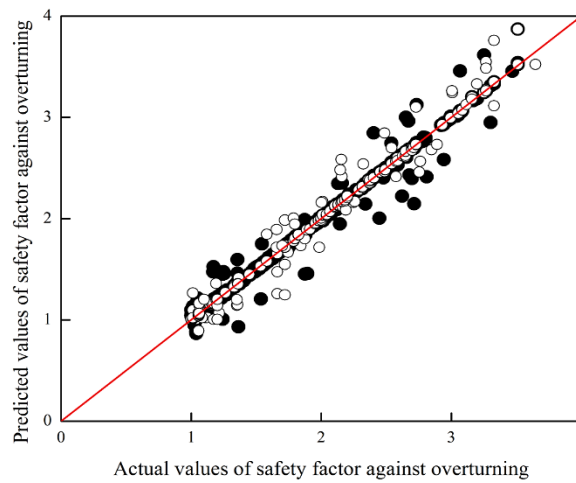


Figure 9. Predicted safety factors against overturning compared to actual values obtained from deterministic stability analyses (undrained conditions)

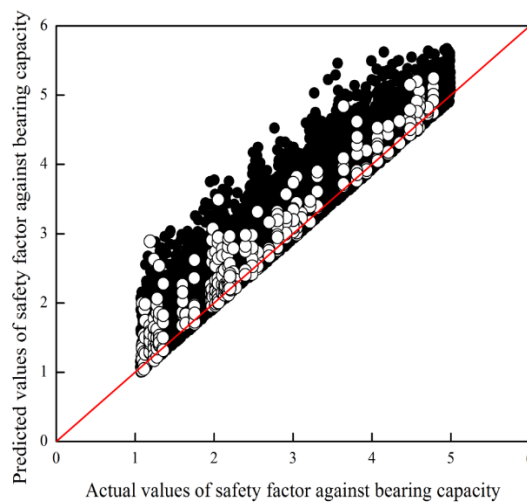


Figure 10. Predicted safety factors against bearing capacity failure compared to the actual values obtained from deterministic stability analyses (undrained conditions)

The results of the sensitivity analysis performed on the safety factors prediction models are presented in Figures 11 to 13. In each graph, one input variable is excluded (by setting its scalar weight to zero) and the ANN model is trained

for the 10 remained input parameters. As it is obvious from the graphs, excluding each parameter causes some extra scatter in the prediction models.

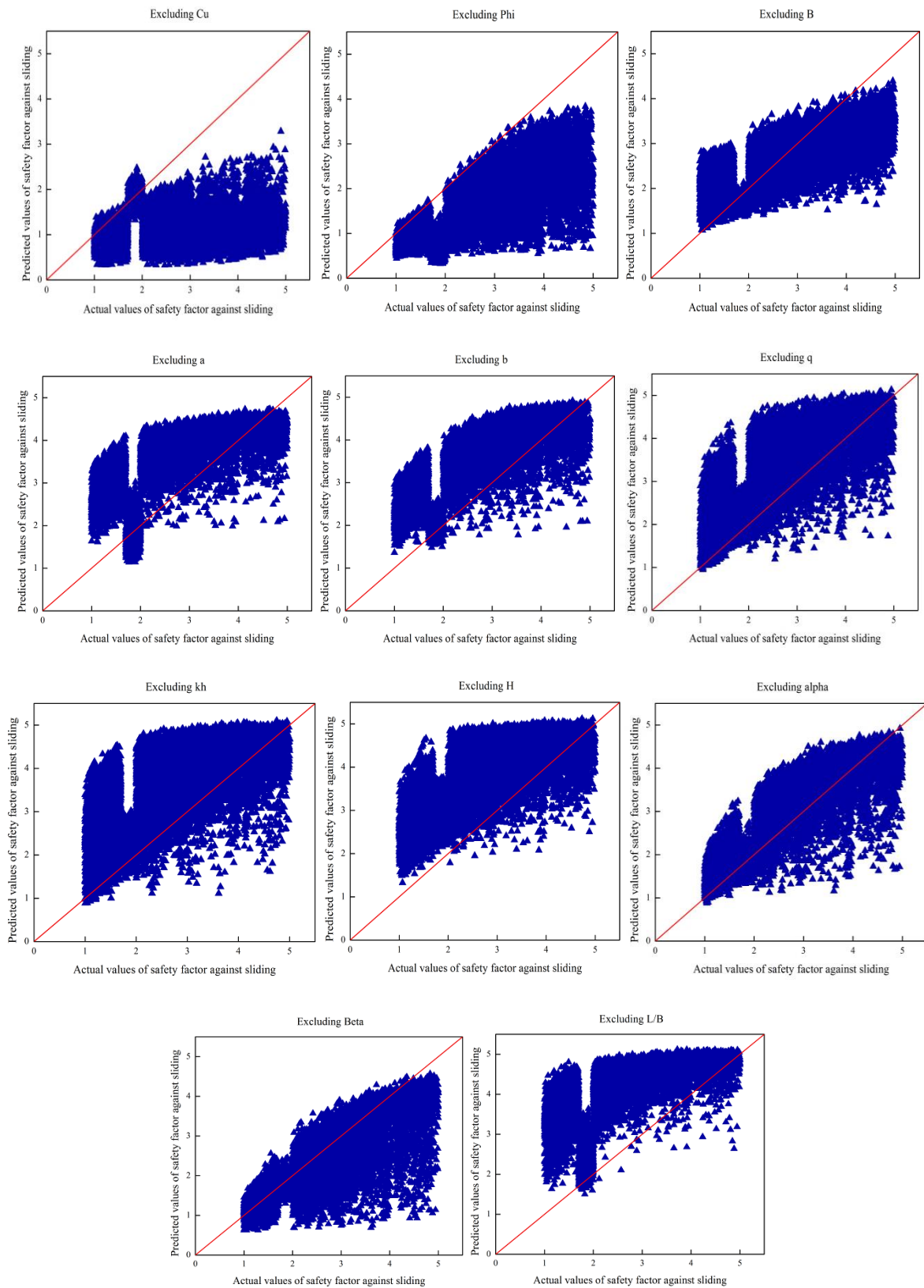


Figure 11. Sensitivity analysis of the sliding safety factor's model (undrained conditions)

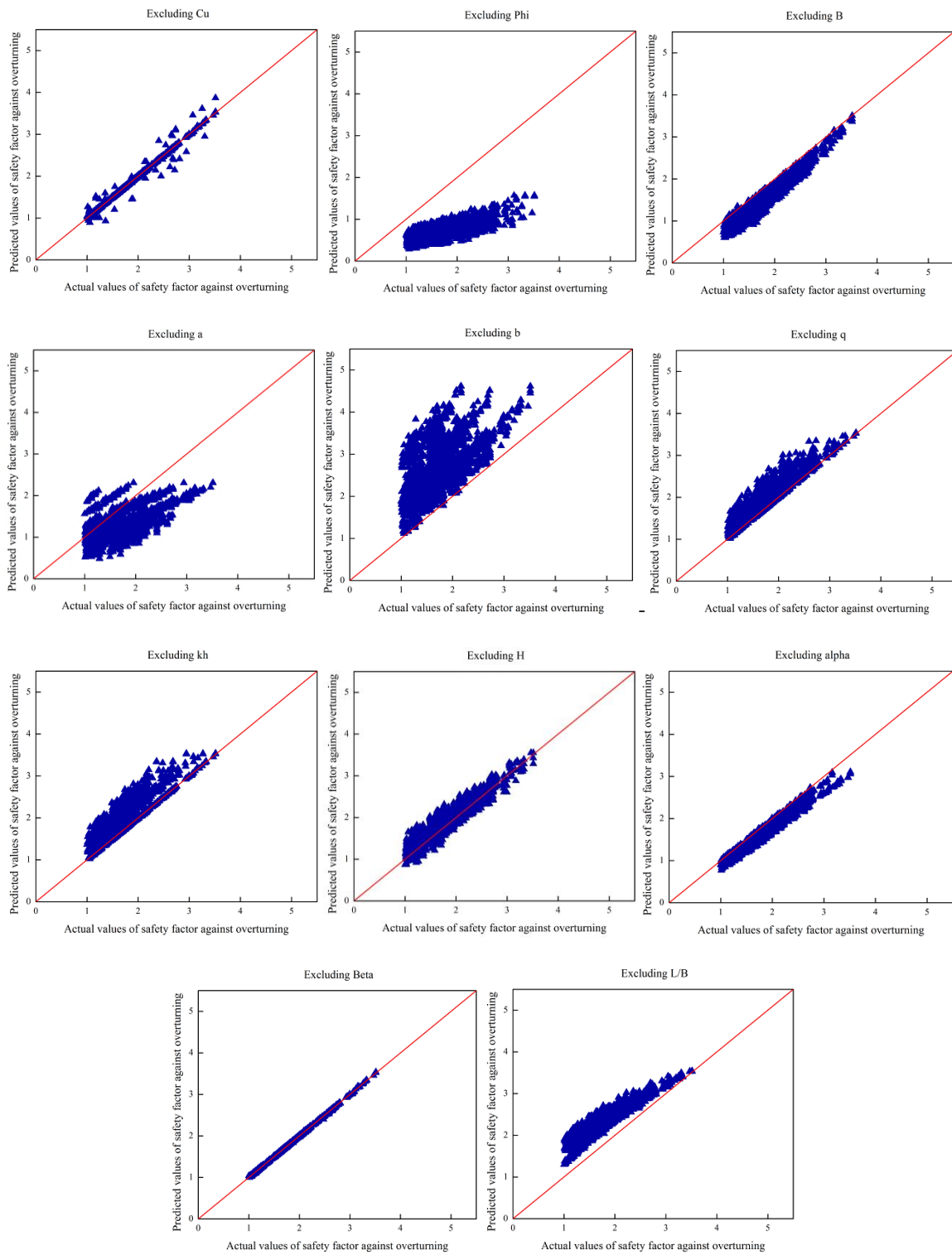


Figure 12. Sensitivity analysis of the overturning safety factor's model (undrained conditions)

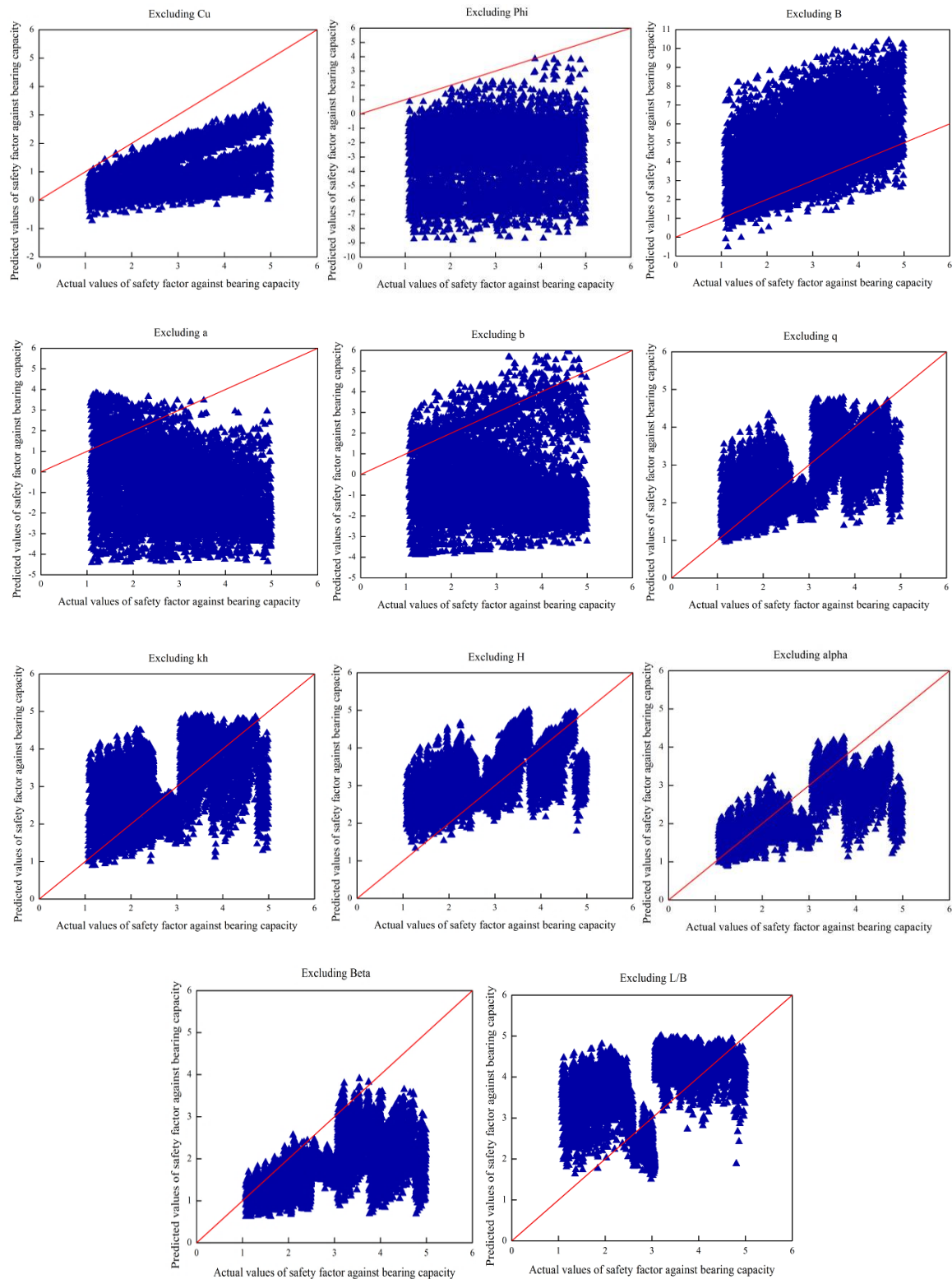


Figure 13. Sensitivity analysis of the bearing capacity safety factor's model (undrained conditions)

Table 2. presents the results of the sensitivity analysis performed on the prediction models. Based on the results, excluding undrained cohesion (C_u) and backfill angle of friction (φ_b) from input parameters cause some scatter in the results. Also in these cases, the high values of CRM indicate the significant role of C_u and φ_b on the ANN performance. It can be seen from Table 2. that the values of $RMSE$ obtained for the bearing capacity failure are considerably higher than the $RMSE$ values obtained for sliding and overturning. The higher $RMSE$ values correspond to the overprediction witnessed in the predicted values of safety factors against bearing capacity failure (Figure 10). This fact points out to the higher accuracy of the models developed for the prediction of the factor of safety against sliding and overturning.

Table 2. Summary of the ANN performance for undrained condition

Outputs		Total	Ex.w ₁ (C _u)	Ex.w ₂ (φ_b)	Ex.w ₃ (B)	Ex.w ₄ (a)	Ex.w ₅ (b)	Ex.w ₆ (q)	Ex.w ₇ (k _h)	Ex.w ₈ (H)	Ex.w ₉ (α)	Ex.w ₁₀ (β)	Ex.w ₁₁ (L/B)
Sliding	COD	0.98	0.01	0.58	0.54	0.48	0.6	0.58	0.42	0.54	0.73	0.66	0.44
	RMSE	0.12	1.83	1.32	0.75	1.11	1.01	0.86	1.18	1.23	0.59	0.68	1.61
	CRM	0.001	0.55	0.42	0.04	-0.3	-0.29	-0.19	-0.31	-0.37	-0.08	0.1	-0.52
Overturning	COD	0.99	0.99	0.48	0.89	0.32	0.36	0.83	0.75	0.85	0.95	0.98	0.8
	RMSE	0.025	0.02	1.03	0.31	0.55	1.04	0.26	0.34	0.19	0.17	0.009	0.57
	CRM	-0.0004	-0.0005	0.57	0.16	0.24	-0.52	-0.09	-0.14	-0.04	0.08	-0.0001	-0.31
Bearing Capacity	COD	0.92	0.27	0.005	0.24	0.07	0.001	0.21	0.11	0.19	0.57	0.85	0.008
	RMSE	0.42	1.97	5.83	2.55	4.25	3.7	1.8	1.08	2.69	0.92	0.45	4.32
	CRM	-0.10	0.62	1.88	-0.68	1.27	1.08	-0.3	-0.33	0.14	0.08	0.05	-1.25

3.2. ANN Prediction Models for Safety Factors of Quay Walls in Drained Conditions

A similar ANN structure with input parameters including friction angle (φ_f), backfill friction angle (φ_b), B, a, b, q, k_h, H, α , β and L/B has been employed to predict the values of the safety factors of the wall in drained conditions.

Figures 14 to 16. show comparisons between safety factors from model training and testing versus the actual data obtained from deterministic stability analyses. It is clear from the graphs that the MLP models give reliable estimation of the safety factors against sliding, overturning and bearing capacity failure.

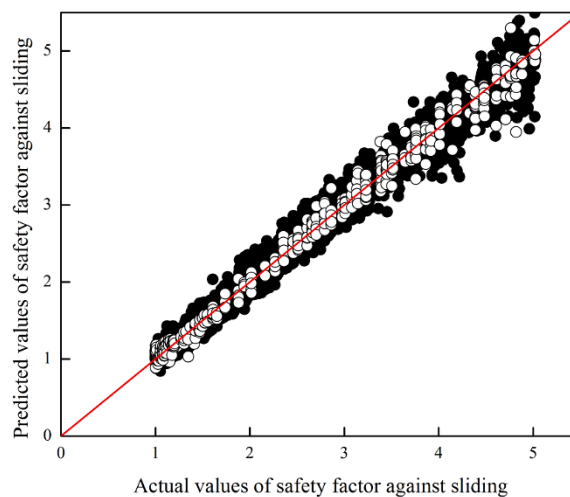


Figure 14. Predicted safety factors against sliding compared to actual values obtained from deterministic stability analyses (drained conditions)

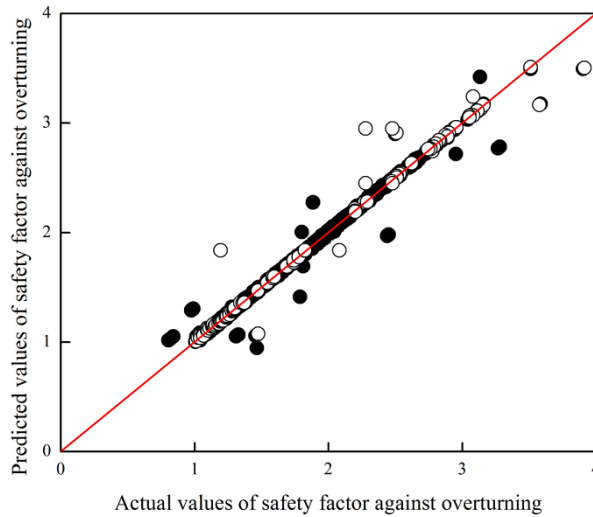


Figure 15. Predicted safety factors against sliding compared to actual values obtained from deterministic stability analyses (drained conditions)

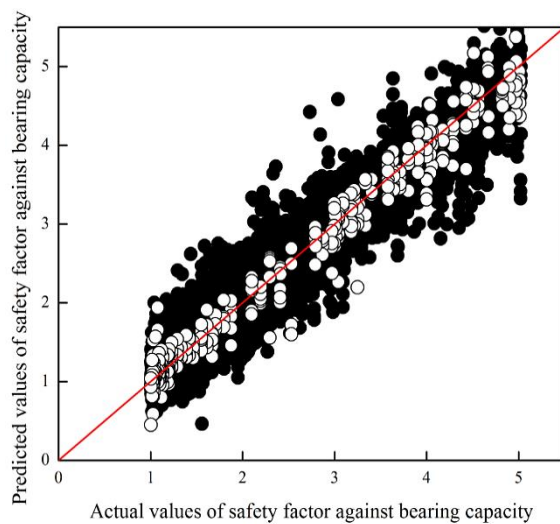


Figure 16. Predicted safety factors against bearing capacity compared to actual values obtained from deterministic stability analyses (drained conditions)

Figures 17 to 19, illustrate the results of the sensitivity analysis performed on the safety factors prediction models. Comparing the graphs illustrates that φ_f and φ_b are the two most important variables in the accuracy of the prediction model.

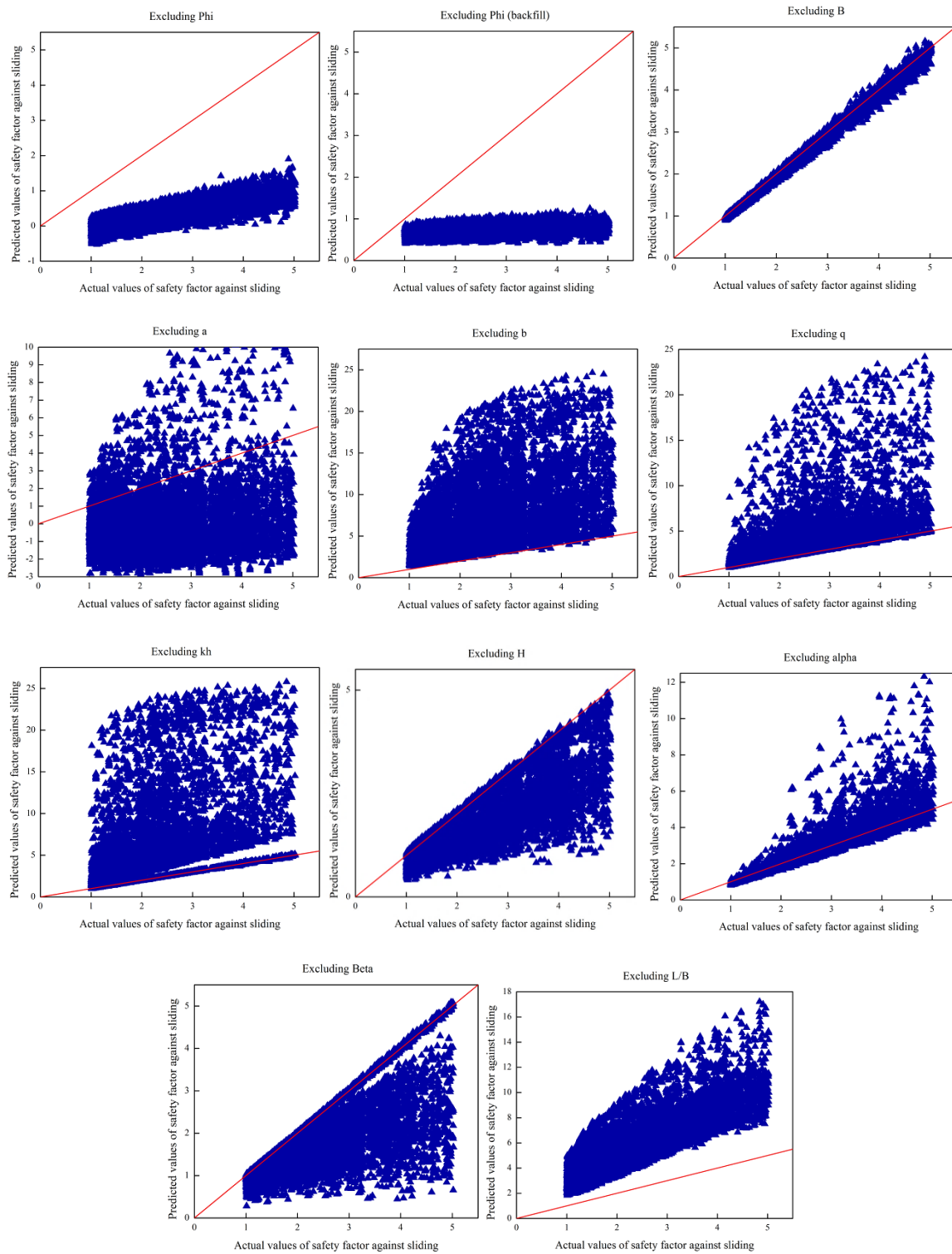


Figure 17. Sensitivity analysis of the sliding safety factor's model (drained conditions)

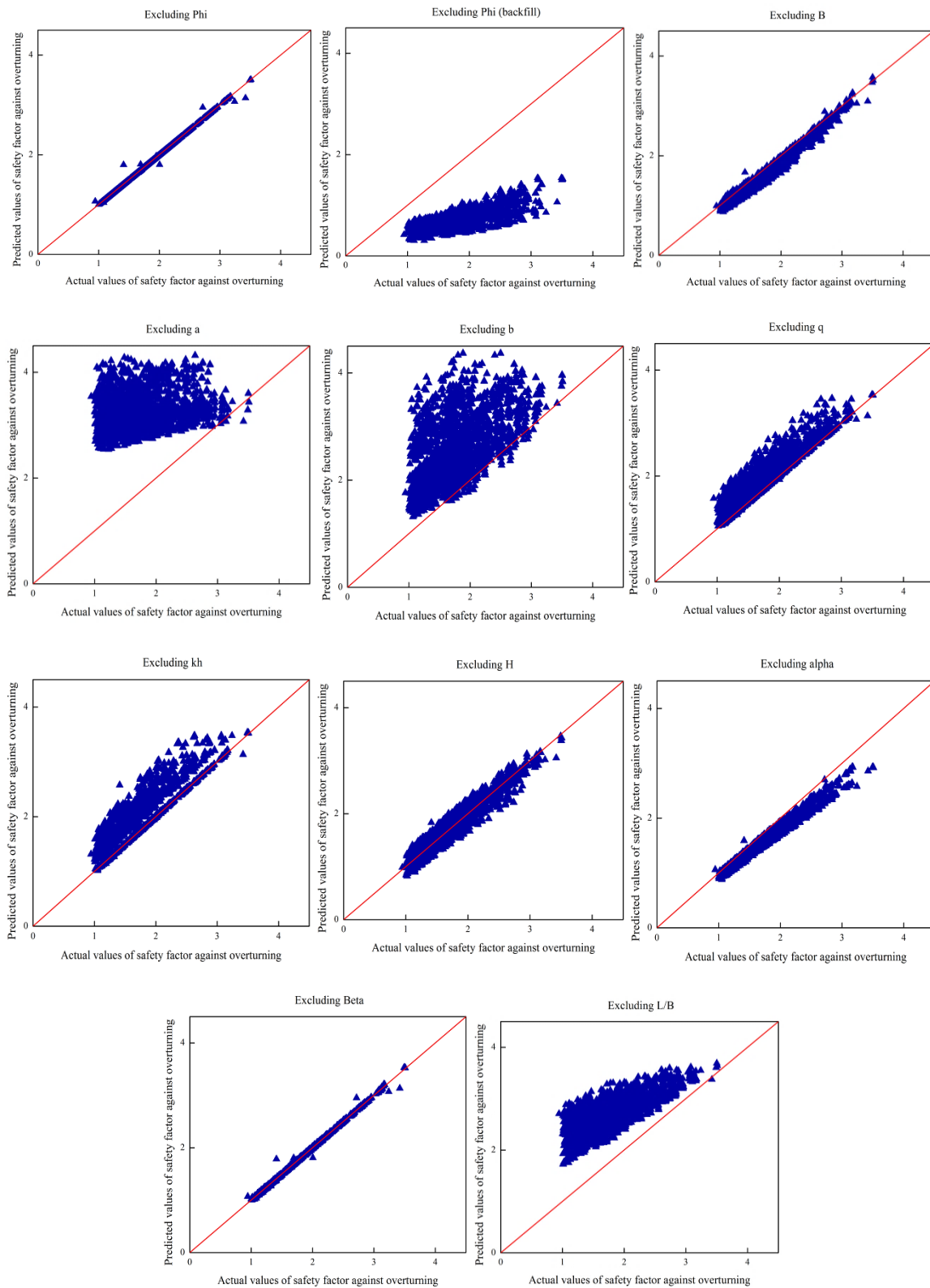


Figure 18. Sensitivity analysis of the overturning safety factor's model (drained conditions)

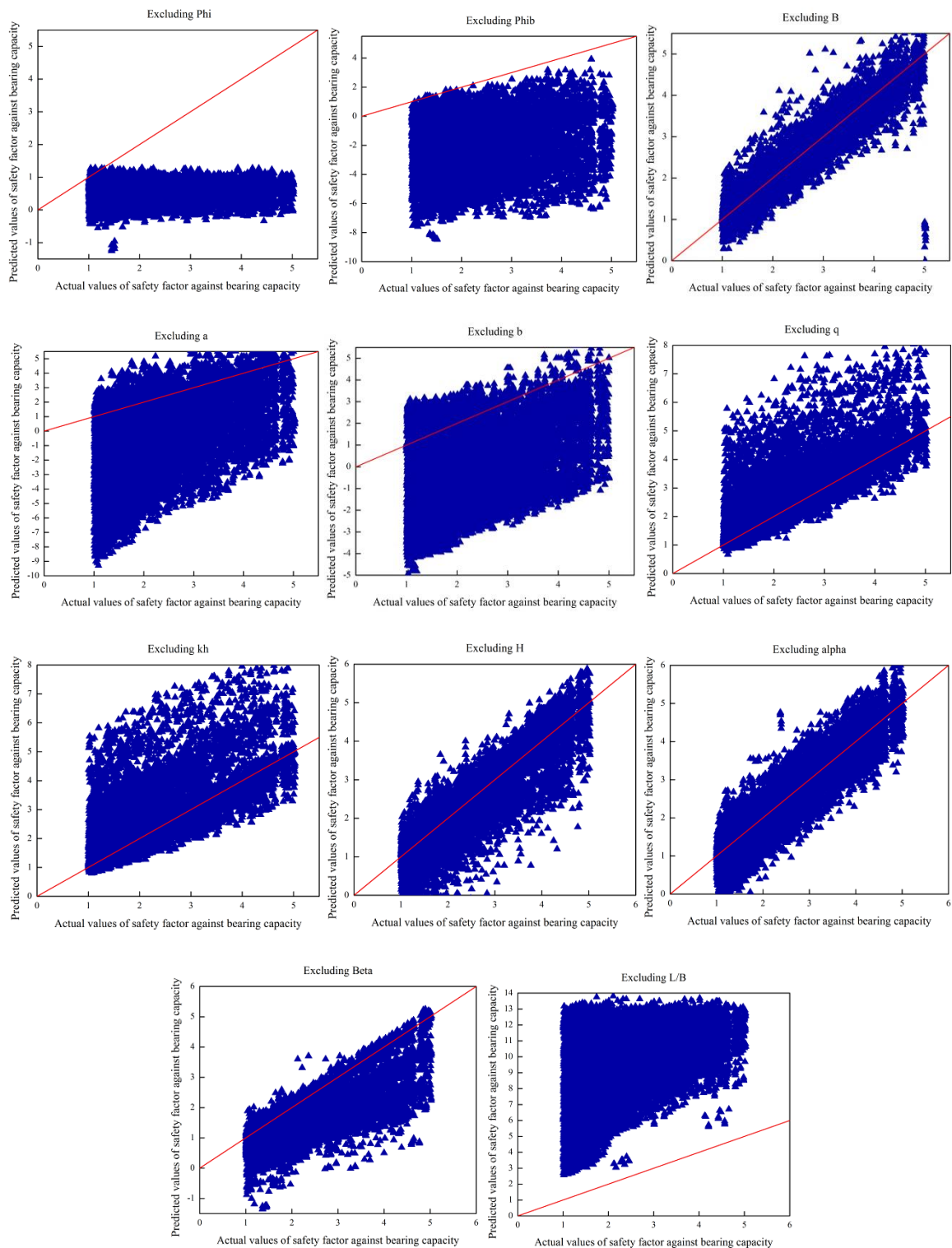


Figure 19. Sensitivity analysis of the bearing capacity safety factor's model (drained conditions)

The performance of the ANN developed models are presented in Table 3. The values of COD, RMSE and CRM illustrate the importance of each input parameter. According to the results, excluding the friction angle (φ_f) causes significant decrease in the accuracy of the developed models. Moreover, the angles of a & b are the other important input parameters. It can also be seen from Table 3. that lower values of RMSE are obtained for overturning compared to sliding and bearing capacity failure which corresponds to the higher accuracy of the model developed for the prediction of factor of safety against overturning seen in Figure 15.

Table 3. Summary of the ANN performance in drained conditions

Outputs		Total	Ex.w1 (φ_f)	Ex.w2 (φ_b)	Ex.w3 (B)	Ex.w4 (a)	Ex.w5 (b)	Ex.w6 (q)	Ex.w7 (kh)	Ex.w8 (H)	Ex.w9 (α)	Ex.w10 (β)	Ex.w11 (L/B)
Sliding	COD	0.98	0.62	0.12	0.98	0.06	0.36	0.34	0.17	0.70	0.82	0.56	0.69
	RMSE	0.101	2.11	1.79	0.09	3.03	4.82	2.61	5.14	0.75	0.58	0.81	3.78
	CRM	-0.0001	0.87	0.67	0.03	1.12	-1.38	-0.5	-1.21	0.23	-0.02	0.21	-1.53
Overturning	COD	0.99	0.98	0.52	0.97	0.04	0.32	0.85	0.77	0.92	0.96	0.98	0.54
	RMSE	0.037	0.37	1.07	0.45	1.77	1.1	0.77	0.38	0.22	0.27	0.54	1.08
	CRM	0.0002	0.02	0.58	0.09	-0.91	-0.46	-0.12	-0.13	-0.02	0.09	-0.02	-0.52
Bearing Capacity	COD	0.95	0.012	0.004	0.91	0.16	0.18	0.62	0.52	0.79	0.84	0.61	0.27
	RMSE	0.22	1.96	4.45	0.32	3.58	3.09	0.85	1.01	0.49	0.43	0.91	6.84
	CRM	0.001	0.74	1.71	0.03	1.15	1.11	-0.16	-0.18	0.03	0.01	0.28	-2.86

4. Conclusion

This paper presents a set of ANN models for predicting the safety factors of quay walls against sliding, overturning and bearing capacity failure. The safety factors of a quay wall are dependent on some geotechnical properties of the backfill soil and the soil beneath such as the cohesion and friction angle. In addition, the drainage conditions and the geometry of the wall are considerably important in the stability of a quay wall.

By introducing these variables in their common range of existence, around 80000 hypothetical cases were created and their stability conditions were estimated using a MATLAB aided program based on OCDI (2000) methodology of quay wall stability analysis.

Results of these analyses were collected as a data bank with the variables effective on the soil-quay wall stability as inputs and three values of calculated safety factors against sliding, overturning and foundation bearing capacity as outputs.

The results of the prediction models have been compared with the actual data. Comparison of the results demonstrates that the developed ANN models provide accurate predictions. A major strength of the ANN prediction models is their ability to improve as more data become available without repeating the development procedures from the beginning.

Furthermore, some sensitivity analyses have been performed to illustrate the influence of each parameter on the ANN performance: such analyses put in evidence the high influence of strength parameters on the results.

5. References

- [1] PIANC (2001), Seismic Design Guidelines for Port Structures, Permanent International Association for Navigation Congresses, Balkema, 474p.
- [2] Sadrekarimi, A., Ghalandarzadeh, A., and Sadrekarimi, J. "Static and dynamic behavior of hunchbacked gravity quay walls." *Soil Dyn. Earthquake Eng.* 28(2) (2008): 99–117.
- [3] Sadrekarimi, A. "Seismic Displacement of Broken-Back Gravity Quay Walls." *Journal of Waterway, Port, Coastal, and Ocean Engineering*, Vol. 137, (2011): No. 2.
- [4] Sadrekarimi, A. "Pseudo-static lateral earth pressures on brokenback retaining walls Seismic Displacement of Broken-Back Gravity Quay Walls", *Canadian Journal of Geotechnical Engineering*, Vol. 47, (2010): 1247–1258
- [5] Technical Standards and Commentaries for Port and Harbour Facilities in Japan, The Overseas Coastal Area Development Institute of Japan (OCDI), (2002): 600P.
- [6] Okabe, S. "General theory of earth pressure and seismic stability of retaining wall and dam". *Journal of the Japanese Society of Civil Engineers*, 10 (5) (1924): 1277–1323.
- [7] Mononobe, N. and Matsuo, M. (1929). On the determination of earth pressures during earthquakes: Proceedings of the World Engineering Congress, Tokyo, Japan. International Association for Earthquake Engineering, Japan. 1929, Vol.9, pp. 177–185.
- [8] Ichihara, M., and Matsuzawa, H. "Earth pressure during earth-quake". *Soils and Foundations*, 13 (4) (1973): 75–86
- [9] Westergaard, H.M. "Water pressure on dams during earthquakes". *Transactions of the American Society of Civil Engineers*, 98

(1933): 418–472.

[10] Goh, ATC. "Nonlinear modeling in geotechnical engineering using neural networks". Aust Civ Eng Trans CE36(4) (1994): 293–297

[11] Ural, D. N., and Saka, H. "Liquefaction assessment by neural networks". Electronic Journal of Geotechnical Engineering. (1998): <http://geotech.civen.okstate.edu/ejge/ppr9803/index.html>.

[12] Najjar, Y. M., and Ali, H. E. "CPT-based liquefaction potential assessment: A neuronet approach". Geotechnical Special Publication, ASCE, 1, (1998): 542-553.

[13] Sivakugan, N., Eckersley, J. D., and Li, H. "Settlement predictions using neural networks". Australian Civil Engineering Transactions, CE40, (1998): 49-52.

[14] Ghiassian, H., Jamshidi, R., and Poorebrahim, G. "Neural networks analysis of silty sand reinforced by carpet wastes" Kuwait Journal of Science and Engineering, (2006): 33(1) pp. 119-139

[15] Sinha, S. K. and Wang, M. C. "Artificial Neural Network Prediction Models for Soil Compaction and Permeability". Geotechnical and Geological Engineering, Vol. 26, Issue 1, (2008): pp 47–64

[16] Gunaydin, O. "Estimation of soil compaction parameters by using statistical analyses and artificial neural networks". Environmental Geology (2009): 57:203

[17] Rezania, M., Javadi, AA. and Giustolisi, O. "An evolutionary-based data mining technique for assessment of civil engineering systems". JEng Comput 25(6) (2008): 500–517.